

# Redshift leverage for the search of GRB neutrinos affected by quantum properties of spacetime

Giovanni Amelino-Camelia,<sup>1,2</sup> Giacomo D’Amico,<sup>3</sup> Vittorio D’Esposito,<sup>1,2</sup> Giuseppe Fabiano,<sup>4,5,6</sup> Domenico Frattulillo,<sup>2</sup> Giulia Gubitosi,<sup>1,2</sup> Dafne Guetta,<sup>7</sup> Alessandro Moia,<sup>1</sup> and Giacomo Rosati<sup>8,9</sup>

<sup>1</sup>*Dipartimento di Fisica Ettore Pancini, Università di Napoli “Federico II”,  
Complesso Univ. Monte S. Angelo, I-80126 Napoli, Italy*

<sup>2</sup>*Istituto Nazionale di Fisica Nucleare, Sezione di Napoli,  
Complesso Univ. Monte S. Angelo, I-80126 Napoli, Italy*

<sup>3</sup>*Department for Physics and Technology, University of Bergen, NO-5020 Bergen, Norway*

<sup>4</sup>*Physics Division, Lawrence Berkeley National Laboratory, Berkeley, CA 94720, USA*

<sup>5</sup>*Department of Physics, University of California, Berkeley, CA 94720, USA*

<sup>6</sup>*Centro Ricerche Enrico Fermi, I-00184 Rome, Italy*

<sup>7</sup>*Capodimonte Observatory, INAF-Naples, Salita Moiariello 16, Naples 80131, Italy*

<sup>8</sup>*Dipartimento di Matematica, Università di Cagliari, via Ospedale 72, 09124 Cagliari, Italy*

<sup>9</sup>*Institute for Theoretical Physics, University of Wrocław,  
Pl. Maksa Borna 9, PL-50-204 Wrocław, Poland*

Some previous studies based on IceCube neutrinos had found intriguing preliminary evidence that some of them might be GRB neutrinos with travel times affected by quantum properties of spacetime delaying them proportionally to their energy, an effect often labeled as “quantum-spacetime-induced in-vacuo dispersion”. Those previous studies looked for candidate GRB neutrinos in a fixed (neutrino-energy-independent) time window after the GRB onset and relied rather crucially on crude estimates of the redshift of GRBs whose redshift has not been measured. We here introduce a complementary approach to the search of quantum-spacetime-affected GRB neutrinos which restricts the analysis to GRBs of sharply known redshift, and, in a way that we argue is synergistic with having sharp information on redshift, adopts a neutrino-energy-dependent time window. We find that knowing the redshift of the GRBs strengthens the analysis enough to compensate for the fact that of course the restriction to GRBs of known redshift reduces the number of candidate GRB neutrinos. And rather remarkably our estimate of the magnitude of the in-vacuo-dispersion effects is fully consistent with what had been found using the previous approach. Our findings are still inconclusive, since their significance is quantified by a  $p$ -value of little less than 0.01, but provide motivation for monitoring the accrual of neutrino observations by IceCube and KM3NeT as well as for further refinements of the strategy of analysis here proposed.

## I. INTRODUCTION AND NEW SELECTION CRITERIA

The current generation of neutrino telescopes was devised to mark the start of neutrino astrophysics, and indeed IceCube firmly established the observation of cosmological neutrinos [1], but so far not much astrophysics has been done with neutrinos: we only have a single case of observation of a source in neutrinos, the case of the active galaxy NGC 1068 for which IceCube reported robust statistical evidence of neutrino observations [2]. With respect to pre-IceCube expectations what is clearly missing are observations of neutrinos from GRBs (gamma-ray bursts): the prediction of a neutrino emission associated with GRBs is generic within the most widely accepted astrophysical models [3] and pre-IceCube studies estimated about a handful of GRB-neutrino observations per year of operation [4–7], but as IceCube nears 15 years of operation still not a single GRB neutrino has been observed. The simplest (and most likely) explanation of this huge underperformance of IceCube is that our GRB models must be revised in such a way to produce a much lower neutrino flux, but it is intriguing that in principle our failure to observe GRB neutrinos could also be attributed to some plausible quantum properties of spacetime which

had already been investigated for independent reasons in the quantum-gravity literature: IceCube searches might have failed to find GRB neutrinos because they assume that GRB neutrinos should be detected in very close temporal coincidence with the associated gamma rays, but a sizable mismatch between GRB-neutrino detection time and the time of detection of the electromagnetic GRB signal would be expected in presence of “in-vacuo dispersion”, a much-studied effect such that quantum properties of spacetime slow down<sup>1</sup> particles proportionally to their energies (see, *e.g.*, Refs. [8–17] and references therein).

We here focus exclusively on the most studied scenario for in-vacuo dispersion which for our purposes is conveniently characterized in terms of the following relationship [18–22]:

$$\Delta t = \eta D(z) \frac{E}{M_P}, \quad (1)$$

<sup>1</sup> While the theoretical prejudice of most quantum-spacetime researchers favours effects that slow down particles, there is no conclusive theoretical argument ruling out that quantum-spacetime effects might instead speed up particles. We offer some data-based observations relevant for this issue in parts of Sec. V.

where  $\Delta t$  is the contribution to the travel time of the neutrino from quantum-gravity-induced in-vacuo dispersion,  $M_P$  denotes the Planck scale ( $\sim 10^{28} \text{ eV}$ ), and  $D(z)$  is a function of the redshift  $z$  of the GRB associated to the neutrino,

$$D(z) = \int_0^z d\zeta \frac{(1 + \zeta)}{H_0 \sqrt{\Omega_\Lambda + (1 + \zeta)^3 \Omega_m}}$$

( $\Omega_\Lambda$ ,  $H_0$  and  $\Omega_m$  denote, as usual, respectively the cosmological constant, the Hubble parameter and the matter fraction, for which we take the values given in Ref. [23]).

We shall mainly focus on the scenario with pure systematic effects, in which  $\eta$  is simply a parameter to be determined experimentally, but in a few points we shall offer remarks relevant for the more general case of a mixture of systematic and fuzzy effects [16, 17, 24], in which  $\eta$  is described as  $\eta_0 + \delta\eta$ , where  $\eta_0$  is a fixed parameter (taking the same value in all neutrino observations) while  $\delta\eta$  is an additional contribution that differs from one instance to another of neutrino observation and vanishes on average.

The effects of Eq.(1) are totally unnoticeable on terrestrial scales, but for the observation of distant astrophysical sources the factor  $D(z)$  can be large enough to compensate for the Planck-scale suppression [8–17].

As observed in some previous studies [18–22, 25, 26] the search of GRB neutrinos affected by in-vacuo dispersion must necessarily rely on a statistical approach: we could never be sure that a certain neutrino is a GRB neutrino, but there is a chance to have at some point a collection of GRB-neutrino candidates (neutrinos that could be associated with a GRB, assuming in-vacuo dispersion) large enough to be sure that at least some of those neutrinos actually are GRB neutrinos, affected by in-vacuo dispersion. This is due to the size of the time window that one must adopt in order to investigate the hypothesis of in-vacuo dispersion. Standard searches of GRB neutrinos (assuming  $\eta = 0$ , no in-vacuo dispersion) can assume that the neutrino and the electromagnetic signal from the GRB travel essentially at the same speed, and therefore their GRB-neutrino candidates are looked for within a tiny time window, rendering background issues insignificant. For  $\eta \neq 0$ , also taking into account that the neutrino energy will have some uncertainty (and however one will inevitably always end up testing an hypothesis of  $\eta$  taking values in a certain range), the difference in observation time between the neutrino and the electromagnetic signal would be sizeably uncertain, and the time window for searches of GRB-neutrino candidates would have to be correspondingly large, resulting in background issues such that one could not be sure that a specific GRB-neutrino association is correct.

Evidently the effectiveness of such a statistical approach depends rather crucially on the criteria used for the selection of candidate GRB neutrinos. And our main objective here is to test a novel proposal for these criteria. Testing alternative strategies of analysis on presently-available IceCube data also acquires additional impor-

tance because it can set the stage for a later, more mature, phase of the research program, eventually using also data from KM3Net [27] and IceCube-Gen2 [28].

Previous searches [18–22, 25, 26] of GRB neutrinos looked for neutrinos within a time window of fixed size (neutrino-energy-independent) after the GRB onset, and put on the same footing both GRBs whose redshift has not been measured (then having to estimate that redshift crudely, since the conjectured effect is redshift dependent) and GRBs of known redshift. Including GRBs whose redshift has not been measured has the advantage of a larger number of candidate GRB neutrinos, but of course renders the analysis vulnerable to the assumptions made to roughly estimate the redshifts. Moreover, the fixed-size time window, while easily handled computationally, imposes a restriction of the analysis to a corresponding limited range of neutrino energies: since the sought effect grows linearly with energy, a time window adapted to energies of, say, 100 TeV will inevitably be too small for neutrinos with energy much greater than 100 TeV, and in an appropriate sense it would also be too large a time window for neutrinos of energy much smaller than 100 TeV (when the time window is much wider than the one really needed by the sought effect, the analysis ends up being dominated by background). In spite of these limitations, Ref. [26], the latest such study (of which some of us were authors), provided the estimate<sup>2</sup>  $\eta = 21.7 \pm 4.5$  with a  $p$ -value  $P_{[26]} = 0.007$ .

We here take the results of Ref. [26] as a starting point for testing a novel strategy of analysis. Rather than adopting a fixed-size time window and correspondingly restricting the neutrino-energy range, we consider all the neutrinos in the sample, regardless of the energy, but restrict the GRB catalogue to GRBs of known redshift. Any GRB and neutrino times of arrival are then regarded as compatible if they satisfy Eq. (1) for some  $\eta \in [12.7, 30.7]$  (the two-standard-deviation interval obtained from the estimate  $\eta = 21.7 \pm 4.5$  found in Ref. [26]) within two standard uncertainties in the neutrino visible energy. As here shown in Sec. IV, the fact that, by relying exclusively on GRBs of known redshift, we find fewer GRB-neutrino candidates is more than compensated, for what concerns the overall statistical significance, by the sharper setup of the analysis which is available when the redshift of the GRBs is known.

Also for what concerns the assessment of the directional compatibility between a neutrino and a GRB the criteria here adopted differ from those of previous analogous studies. This change, however, does not reflect

---

<sup>2</sup> As it will be clearer for our readers when, later in this manuscript, we derive an analogous  $p$ -value for our novel selection criteria, this  $p$ -value, which in [26] was called false alarm probability, is the probability that all the found GRB-neutrino candidates actually are background neutrinos (probability of no signal), while  $\eta = 21.7 \pm 4.5$  is the estimate of  $\eta$  obtained from the found GRB-neutrino candidates.

a strategic choice: it is rather due to a qualitative upgrade in the neutrino directional information provided by IceCube. Previous IceCube data releases provided directional information in terms of approximate gaussian uncertainties, whereas the latest data release characterizes the uncertainty in the direction of a neutrino in terms of an 8-parameter Fisher-Bingham (FB8) distribution on the sphere [29]. The asymmetry and complexity of this distribution makes it impossible to reduce the assessment of its directional compatibility with the directional PDF of a known-redshift GRB to a straightforward comparison of their most probable values, as done, *e.g.*, in [26]. Rather, we follow other studies that handled similarly complex directional uncertainties (see, *e.g.*, Ref. [30]) and rely on the value of the statistic  $\mathcal{S} = \int P_\nu(\Omega)P_{GRB}(\Omega)d\Omega$ , where  $P_\nu(\Omega)$  and  $P_{GRB}(\Omega)$  are the angular distributions of the neutrino and the GRB, respectively. This  $\mathcal{S}$  can be computed for angular distributions of arbitrary shape and is a good measure [30] of angular compatibility (in particular, its value increases as the peaks of the two distributions grow closer). We thus regard the directions of a GRB-neutrino pair as compatible if the corresponding  $\mathcal{S}$  satisfies  $\mathcal{S} \geq \mathcal{S}_{cut}$  for some fixed reference value  $\mathcal{S}_{cut}$ . In setting up our study we adopted  $\mathcal{S}_{cut} = 1/4\pi$ , which is the value taken by  $\mathcal{S}$  whenever one of the distributions is the uniform distribution on the sphere. This choice is intuitively natural, as it would be difficult to claim any degree of directional compatibility if two uniform, uninformative distributions would be given a better score. In any case, after performing our main analysis (here reported in Sec. IV), we explored the dependence of our results on the choice of  $\mathcal{S}_{cut}$ , finding that it is rather weak (see Sec. V).

## II. ICECUBE NEUTRINOS AND GRBS OF KNOWN REDSHIFT

Our analysis relies on the latest HESE data release by IceCube (7 September 2023), available at [31]. As done in previous analogous studies [18–22, 26], we restrict to shower events, since track events have very poor energy estimates (and of course the quality of the energy information is crucial for in-vacuo-dispersion studies) [40, 42].

A sizable part of the effort we devoted to this study was aimed at compiling a reliable catalogue of GRBs with actually measured (and not just estimated or loosely constrained) redshifts. In fact, we found that all already available GRB catalogues either imposed further constraints on the GRB properties (narrower observation window, restriction to specific GRB observatories, GRB type, etc.) or were not sufficiently accurate (misreporting or omitting direction or redshift data, not taking into account the latest relevant GCNs, etc.). The resulting list is reported here in Appendix A. In about 90% of cases it agrees with an analogous general-purpose catalogue, not restricted to known-redshift GRBs, maintained by the IceCube collaboration [32]. The previous study [26] re-

lied on this resource, but, after checking one-by-one each of its known-redshift entries, we noticed that some of the information relevant for our analysis was inaccurately reported, probably due to the automated population of the database. In most cases this was quickly corrected according to the web catalogue [33] maintained by Jochen Greiner at the MPE, which we found to be the most accurate and comprehensive among publicly available lists. Checking by hand all the relevant GCNs and consulting additional catalogues of known-redshift GRBs, we were then able to correct the few errors left and also identify a few known-redshift GRBs whose redshift is not reported in Greiner’s table (see Appendix A for details).

In the end, all these efforts did not actually pay off in terms of a significant improvement of our analysis: as regards the four GRBs of known redshift playing a crucial role in our main analysis (see Sec. IV), our corrected and augmented catalogue agrees with both [32] and [33]. Still, we hope that the effort we put in preparing Appendix A will be of service to the community. In particular, our Appendix A should represent a tangible improvement over both [32] and [33] for researchers exploring alternative search strategies for GRB neutrinos affected by in-vacuo dispersion.

## III. SIMULATED DATA FOR THE STATISTICAL-SIGNIFICANCE ANALYSIS AND BACKGROUND ESTIMATE

As stressed above, the in-vacuo-dispersion significance of our findings can only be investigated using a statistical approach based on the *p*-value, *i.e.* estimating numerically the probability that one could find GRB-neutrino candidates in such good agreement with the in-vacuo-dispersion hypothesis just by accident, as an outlier of the type of findings one would expect within the null hypothesis  $\eta = 0$  of no in-vacuo dispersion.

As done in the previous neutrino studies<sup>3</sup> of Refs. [18–20], we do this by producing simulated data through transformations of the real data which reliably preserve their morphology while washing away any possible correlations of the type predicted by Eq.(1) between the times of arrival, the neutrino energy, and  $D(z)$ .

Our simulated data are obtained from the real data performing the following independent manipulations:

- we act on the neutrino observation times with a random permutation and a random periodic time translation (the periodicity makes it sure that they stay within the actual IceCube observation window);
- we act on the neutrino directions with a random rotation around the Earth’s axis;

<sup>3</sup> The interested reader can find applications of this method of statistical analysis to studies not involving neutrinos, *e.g.*, in Refs. [30, 34–38].

- we act on the GRB directions with a random permutation and a random rotation around the Galactic axis.

A combination of these manipulations is arguably the most general transformation of the true data not affecting their morphology in any relevant respect. In fact:

- the neutrino observation times are statistically compatible with their being uniformly distributed within the IceCube observation window, and there are no a-priori reason for expecting a change in the HESE neutrino rate in this period;
- the efficiency of the IceCube detector, whose axis is closely aligned to the Earth’s axis, is virtually independent of the right ascension, but not of the declination, of incoming neutrinos, as clearly evidenced in the neutrino angular data; we choose not to reshuffle the neutrino directions so as not to spoil their evident correlation with the neutrino energies (the higher the neutrino energy, the more accurate its reconstructed direction);
- the directions of known-redshift GRBs are independent of galactic longitude, but are correlated to some extent with galactic latitude, as the dust lying around the galactic plane makes it much more difficult to determine the redshift of a GRB in that region; also, we do not act on the GRB observation times because we find that the detection rate of known-redshift GRB is declining with time, probably another selection effect due to older events having been more likely followed by the long-term, host-galaxy observations which are often needed to determine the redshift of a GRB.

As a first application of our simulated data we can estimate the background that is expected with the criteria adopted by our strategy of analysis. For this purpose, we generated  $10^5$  instances of simulated data and we used them to estimate the expected number of background neutrinos that would accidentally be associated with a GRB according to the time-energy and direction compatibility conditions specified above ( $\eta \in [12.7, 30.7]$  and  $\mathcal{S}_{cut} = 1/4\pi$ ). We find that, on average, our criteria should pick up 1.02 background neutrinos.

#### IV. MAIN ANALYSIS

Equipped with the preparatory work reported in the previous sections, we are now ready to discuss our main analysis. We begin by looking for GRB-neutrino candidates, using the data described in Sec. II. For each GRB-neutrino pair selected by our directional criteria ( $\mathcal{S} > 1/4\pi$ ) we describe the  $\Delta t$  of Eq.(1) as the difference between the neutrino observation time<sup>4</sup> and the observation time of the GRB, which we label as  $\Delta t_{candidate}$ ,

<sup>4</sup> If there was no in-vacuo dispersion, a GRB neutrino would be observed (nearly-)simultaneously with the GRB photons. We attribute the whole of the time-of-arrival difference to the  $\Delta t$  of the neutrino, since photons observed from GRBs are of much lower energies than our neutrinos and the effect we are studying depends linearly on energy. Some quantum-spacetime scenarios

and then we use Eq.(1) and the known redshift of the GRB, which we label as  $z_{GRB}$ , to convert the requirement that  $\eta$  should be within the interval  $[12.7, 30.7]$  into a corresponding range of allowed values for the neutrino energy. We then consider the GRB-neutrino pair a “GRB-neutrino candidate” if the energy of the neutrino is compatible with that energy range within two standard deviations (assuming 10% uncertainty in the energy of the neutrino [40]). We find that there are four such GRB-neutrino candidates. Fig. 1 provides a visual characterization of the fact that the properties of these four GRB-neutrino candidates match rather well the expectations of the in-vacuo-dispersion scenario of Eq. (1).

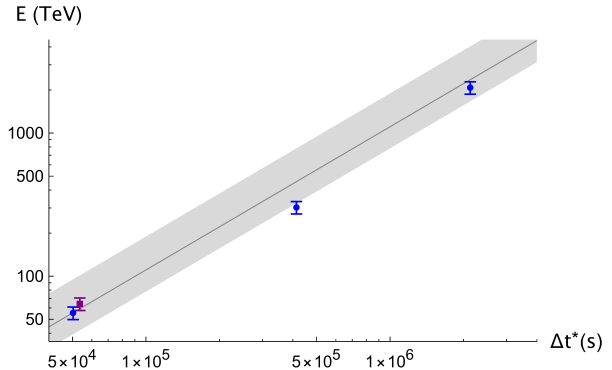


FIG. 1. The values of  $E$  and  $\Delta t^*$  of our four GRB-neutrino candidates line up rather nicely according to the expectations of in-vacuo dispersion. Only one of them, here shown as a violet square, was taken into account also in the analysis of Ref. [26]. The content of this figure should be assessed also keeping in mind the results here reported in Sec. III, suggesting that it is likely that one of our four GRB-neutrino candidates is background. Based on the estimate  $\eta = 21.7 \pm 4.5$  reported in Ref. [26], the dark-gray line corresponds to  $\eta = 21.7$ , while the light-gray band highlights our region of interest in the  $E$ - $\Delta t^*$  plane, corresponding to  $\eta \in [12.7, 30.7]$  via Eq.(1) (see Sec. I for comments on this interval).

In Fig. 1,  $\Delta t^*$  is defined as

$$\Delta t^* \equiv \frac{D(1)}{D(z_{GRB})} \Delta t_{candidate}$$

(the numerical factor  $D(1)$  is introduced only for the convenience of having a  $\Delta t^*$  with dimensions of time), and according to Eq.(1) one should find a linear relationship between  $E$  and  $\Delta t^*$ ,

$$\Delta t^* = \eta D(1) \frac{E}{M_P}.$$

predict in-vacuo dispersion with different magnitude for photons and neutrinos (and if the magnitude was much stronger for photons this assumption of our analysis would not be satisfied); it is however noteworthy that effective-field-theory approaches to quantum properties of spacetime predict that the type of pure in-vacuo dispersion here studied is actually forbidden for photons whereas it is allowed for neutrinos [15, 39].

It is clearly encouraging for the hypothesis of in-vacuo dispersion that our criteria find four GRB-neutrino candidates (some details on these four GRB-neutrino candidates are provided in Appendix B), whereas according to the pure-background null hypothesis we expected to typically find only one (see Sec. III). Further encouragement comes from the fact that in Fig. 1 our four GRB-neutrino candidates line up rather nicely, as measured by their correlation coefficient  $r(\Delta t^*, E) = 0.9985$ . In particular, three of the four GRB-neutrino candidates are compatible with a remarkably narrow range of values of  $\eta$ , an observation which strengthens the appeal of the conjecture that three of our four GRB-neutrino candidates actually might be GRB neutrinos affected by in-vacuo dispersion.

The fact that our findings reported in Fig. 1 fit very well with the estimate  $\eta = 21.7 \pm 4.5$ , which resulted from the analysis of Ref. [26], is noteworthy since, because of the different criteria adopted for the selection of GRB-neutrino candidates, the two analyses only share one GRB-neutrino candidate, the one shown as a violet square in Fig. 1. The analysis leading to the estimate  $\eta = 21.7 \pm 4.5$ , in Ref. [26] ended up focusing on seven GRB-neutrino candidates, but only one of them involved a GRB whose redshift has been measured.

It is of course necessary to quantify statistically this observation that the data we are analyzing match well the expectations of in-vacuo dispersion. For this purpose we rely on the same strategy of characterization of statistical significance adopted in Ref. [26]. In parts of the next Section we shall contemplate alternative strategies of characterization of statistical significance, but the main objective of the study we are here reporting is to compare the GRB-neutrino-candidate selection criteria here adopted with the selection criteria adopted in Ref. [26], and this comparison is of course more transparent if the two selection strategies are assessed using the same characterization of statistical significance. The main analysis of Ref. [26] focused on seven GRB-neutrino candidates and established how frequently simulated data produced at least seven GRB-neutrino candidates with correlation at least as high as the correlation of the GRB-neutrino candidates found in the true data. This happened in about 0.7% of the trials, yielding the above-mentioned  $p$ -value  $P_{[26]} = 0.007$ . Proceeding in an analogous way with the selection criteria here adopted, we start by using our simulated data (Sec. III) to estimate how frequently the null hypothesis of no in-vacuo dispersion ( $\eta = 0$ ) would produce at least four GRB-neutrino candidates according to our new selection criteria, finding a  $p$ -value  $P_n = 0.019$ . We then proceed to estimate how frequently the null hypothesis would accidentally exhibit at least four GRB-neutrino candidates with correlation  $r(\Delta t^*, E) \geq 0.9985$ , finding a  $p$ -value  $P_r = 0.006$  (which corresponds to a  $2.8\sigma$  significance in Gaussian statistics).

## V. AVENUES FOR REFINING THE STRATEGY OF ANALYSIS

We consider as our main result the  $p$ -value  $P_r = 0.006$  derived in the previous Section, which, while being still far from conclusive, testifies to the discovery potential of the novel GRB-neutrino-candidate selection criteria here advocated, which was our main objective.

In this Section we discuss and investigate some observations which could be used to refine the strategy of analysis. We believe that some of the observations reported in this Section deserve being considered in setting up in-vacuo-dispersion analyses of future neutrino data, even though the quantitative aspects of this Section should be assessed with caution since they were produced in a second phase of our investigations after seeing the data, and might therefore be affected by the sources of bias that are well known for unblind analyses. In particular, some of the observations reported in this Section are at least in part inspired by the fact that we saw that among our four GRB-neutrino candidates there are three that are described particularly well according to Eq. (1), and by our perception that the procedure used in Sec. IV to estimate the significance of our findings did not “benefit” sufficiently from the noteworthy properties of those three best GRB-neutrino candidates.

### A. Alternative choices of $\mathcal{S}_{cut}$

In planning our study we ended up adopting the rather prudent criterion of directional consistency characterized by the intuitively natural choice  $\mathcal{S}_{cut} = 1/4\pi$  (see Sec. I). After completing our main analysis we perceived the need to quantify how frequently this criterion was picking up accidental directional associations between a neutrino and a GRB. Using our simulated data, we checked that the choice  $\mathcal{S}_{cut} = 1/4\pi$  entails a 7.8% probability of accidental directional association between a neutrino and a GRB, which is of course partly responsible for the (large but) tolerable expectation that about one background GRB-neutrino candidate should be accidentally picked up by our overall selection criteria (see Sec. III).

We then checked how strongly the  $p$ -value  $P_r$ , which we regard as our main result, depends on the choice of  $\mathcal{S}_{cut}$ . Fig. 2 shows the dependence of  $P_r$  on  $\mathcal{S}_{cut}$  for  $\mathcal{S}_{cut} \in [0.032, 0.241]$ . The rationale for exploring this particular range of values is that, as checked using our simulated data,  $\mathcal{S}_{cut} = 0.241$  entails a 4.5% probability of accidental directional association, the nominal “two standard deviation” reference, whereas  $\mathcal{S}_{cut} = 0.032$  corresponds to a 10% probability of spurious association. As clearly evidenced by Fig. 2, our main result  $P_r$  does not depend strongly on the choice of  $\mathcal{S}_{cut}$ . It is potentially intriguing that for values of  $\mathcal{S}_{cut}$  just below  $1/4\pi$  we would have found an even smaller  $P_r$ , but, in keeping with the considerations of Sec. I, we currently regard this circumstance as a mere numerical accident occurring

with the presently-available data (rather than a hint for optimizing the analysis of future data).

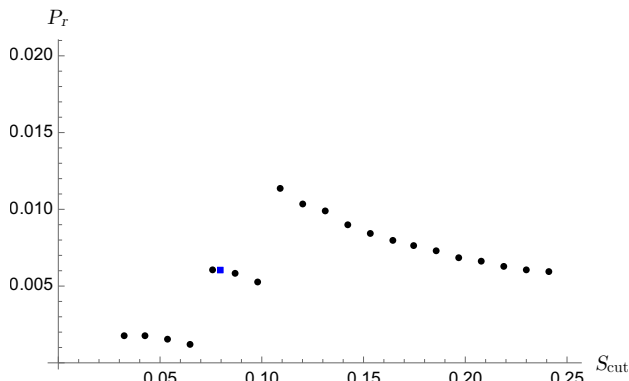


FIG. 2. The  $p$ -value  $P_r$  (see Sec. IV for the definition) as a function of  $S_{cut}$ . The blue square corresponds to the choice  $S_{cut} = 1/4\pi$  of Sec. IV.

### B. Improved correlation

One challenge whose handling might require further methodological refinements in future studies concerns the choice of an appropriate statistic quantifying the agreement between the properties of the found GRB-neutrino candidates and Eq. (1). Investigations of this aspect should take into account the fact that the time window for in-vacuo dispersion searches of GRB neutrinos will always be rather large, even if, as one might hope, the  $\eta$  range on which one would focus could become narrower with the accrual of more data. A relatively small uncertainty on  $\eta$  still translates (especially at high neutrino energies and high redshift) into a rather large time window, large enough for a tangible probability of background contamination of the GRB-neutrino candidates. These concerns are even more severe if one allows for non-systematic fuzzy in-vacuo dispersion effects of the type mentioned here briefly in Sec. I (and discussed in more detail in, *e.g.*, Refs. [16, 17, 24]), since in that case searches of GRB-neutrino candidates would always have to explore a range of  $\eta$  with width at least  $\delta\eta$ .

Awareness of these issues should encourage investigations aimed at quantifying the agreement between the found GRB-neutrino candidates and the relevant in-vacuo-dispersion models in ways that are both robust against contamination by the background and capable of profiting from all the implications of in-vacuo-dispersion.

In our main analysis, reported in Sec. IV, we followed Ref. [26] and characterized the agreement between our findings and Eq. (1) in terms of the standard (Pearson) correlation coefficient  $r(\Delta t^*, E)$ . However,  $r$ , while giving an appropriate weight to the linear relationship between  $E$  and  $\Delta t^*$  predicted by Eq. (1), is completely insensitive to the fact that, according to Eq. (1), one should

have  $\Delta t^* \rightarrow 0$  for  $E \rightarrow 0$ . We observe that this shortcoming can be remedied by replacing the sample covariance and the sample variances appearing in the definition of  $r$  with the corresponding raw (non-central) sample moments, *i.e.*, by replacing  $r(\Delta t^*, E)$  with the corresponding non-central correlation coefficient

$$r_0(\Delta t^*, E) = \frac{\sum_i \Delta t_i^* E_i}{\sqrt{\sum_j (\Delta t_j^*)^2 \sum_k E_k^2}}.$$

It is clear that  $r_0$  indeed rewards GRB-neutrino candidates fitting the expectation that  $E$  depends linearly on  $\Delta t^*$  with negligible intercept.

We can test the effectiveness of this improved statistic by replacing  $r$  with  $r_0$  in our main analysis (Sec. IV). Our four GRB-neutrino candidates have  $r_0(\Delta t^*, E) = 0.9989$ , and requiring that our simulated data (Sec. III) accidentally produce at least four GRB-neutrino candidates with  $r_0(\Delta t^*, E) \geq 0.9989$ , we find a  $p$ -value  $P_{r_0} = 0.004$ .

The fact that  $P_{r_0} < P_r$  suggests that our GRB-neutrino candidates are indeed consistent with the expectation that  $\Delta t^* \rightarrow 0$  for  $E \rightarrow 0$ .

### C. Taking into account the background estimate

Regardless of the statistic used to quantify the agreement of the found GRB-neutrino candidates with Eq. (1), one could also try to tame background contamination by taking explicitly into account its contribution before computing the statistic.

Looking at the GRB-neutrino candidate with  $E = 302$  TeV in Fig. 1, one can easily understand these concerns: even though we expect that one of our four GRB-neutrino candidates should be background, in our main analysis (following Ref. [26]) we computed the correlation coefficient of all of them. Future studies might thus contemplate the possibility of taking into account the background estimate. More explicitly, if one finds  $N$  GRB-neutrino candidates and estimates that there is a large probability, *e.g.*, 90%, that at least  $M$  should be background, it may be appropriate to assess the agreement between the found GRB-neutrino candidates and Eq. (1) using only the best  $N - M$  candidates.

In the case of the study here reported, the probability of finding at least one background candidate is still too low (about 60%) to justify disregarding our worst candidate. Nevertheless, for mere illustrative purposes, we briefly discuss how to amend our main analysis if one of our four candidates could be actually ignored. First, we compute the correlation coefficients of all possible choices of three of our four GRB-neutrino candidates and find that the highest correlation is  $r(\Delta t^*, E) = 0.999997$  (found indeed excluding the candidate with  $E = 302$  TeV). We then use our simulated data to estimate how frequently the null hypothesis would accidentally produce at least four GRB-neutrino candidates such that

three of them have correlation  $r(\Delta t^*, E) \geq 0.999997$ , finding a  $p$ -value  $P_{rb} = 0.002$ .

#### D. Scanning a range of values of $\eta$

The fact that we are restricting our analysis to GRBs with measured redshift allows us to explore another statistic, which we expect to be less vulnerable than correlation to background contamination.

For simplicity we illustrate and discuss the strategy of analysis based on this alternative statistic applying it directly to the data already analyzed in this paper. For every given value of  $\eta$  in our interval of interest [12.7, 30.7], we find the number  $N(\eta)$  of GRB-neutrino candidates which are directionally compatible in the usual sense ( $\mathcal{S} \geq 1/4\pi$ ) and satisfy Eq. (1) for that specific value of  $\eta$  within two standard uncertainties in the neutrino energy. We then use simulated data to estimate the probability that the null hypothesis would accidentally produce at least  $N(\eta)$  such GRB-neutrino candidates, finding a corresponding  $p$ -value  $p(\eta)$ . The resulting “ $p$ -curve” is reproduced here as Fig. 3.

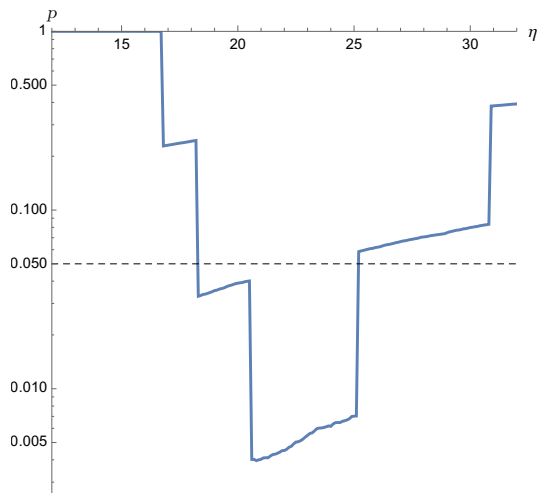


FIG. 3. The  $p$ -curve for  $\eta \in [12.7, 30.7]$ . It is obtained estimating how frequently simulated data produce at least the same number of GRB-neutrino candidates as the real data for each value of  $\eta$  (see text for details). The horizontal dashed line is drawn at  $p = 0.05$ .

Consistently with the fact, already visible in Fig. 1, that our four GRB-neutrino candidates are remarkably compatible with a narrow range of values of  $\eta$ , we see that the  $p$ -curve of Fig. 3 shows a deep valley surrounded by considerably higher values of  $p$ . In particular,  $p(\eta)$  is less than 0.05 (marked as a dashed horizontal line in Fig. 3) for  $\eta \in [18.3, 25.1]$ . The minimum of the  $p$ -curve is found at  $\eta = 20.8$ , fully consistent with the estimate  $21.7 \pm 4.5$  reported in Ref. [26].

The statistical significance of our  $p$ -curve can be characterized estimating how frequently the minimum of

the analogous  $p$ -curves built out of simulated data happens to be less than or equal to the minimum value  $p(20.8) = 0.004$  attained in Fig. 3. The resulting  $p$ -value is  $P_{ns} = 0.012$ .

#### E. Exploring $\eta$ outside the range [12.7, 30.7]

In our main analysis we let  $\eta$  vary in the range [12.7, 30.7] favored by the previous study [26], which adopted different selection criteria, obtaining results in remarkable agreement with those of Ref. [26]. Still, it is interesting to check whether our new GRB-neutrino-candidate selection criteria would have yielded even stronger results for values of  $\eta$  outside the range [12.7, 30.7]. A natural way of doing this is to extend the domain of the  $p$ -curve introduced in the previous Subsection. In Fig. 4 we show the  $p$ -curve for  $\eta \in [-50, 50]$ .

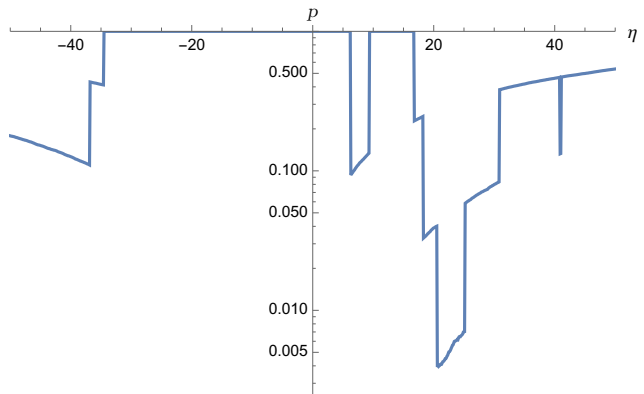


FIG. 4. The same  $p$ -curve of Fig. 3 for  $\eta \in [-50, 50]$ .

Looking at Fig. 4, it is clear that also our new GRB-neutrino-candidate selection criteria favor the range [12.7, 30.7] for  $\eta$ . The fact that we find no other values of  $\eta$  with comparable  $p(\eta)$  is also potentially significant for a much-studied effective-field-theory description of quantum-spacetime properties [39, 41], which in principle allows independent in-vacuo-dispersion parameters for the two neutrino helicities. The prevalent theoretical prejudice is that the two helicities should have the same in-vacuo-dispersion parameter, but it has also been argued that the two helicities might have  $\eta$  with the same modulus but opposite sign [18, 21]. The  $p$ -curve reproduced in Fig. 4 clearly does not provide any encouragement for this helicity-dependence scenario.

## VI. OUTLOOK

The essential equivalence of the  $p$ -values  $P_{[26]}$ , characterizing the statistical significance of the previous analysis [26], and  $P_r$ , found here in Sec. IV and characterizing in the same way the significance of our current analysis, shows that the new, redshift-based selection criteria



for GRB-neutrino candidates proposed in Sec. I are competitive with the ones adopted in Ref. [26]. This means that the improvement in data quality provided by the knowledge of the GRB redshifts is more than sufficient to compensate for the loss of most of the GRB dataset (we measure the redshift of about 1/10 of observed GRBs). We feel that this is our main result, as it effectively opens up a new avenue, complementary to the approach pursued in Ref. [26], to investigate in-vacuo dispersion with neutrinos.

Considering the very significant differences in their selection criteria (as stressed above, only one GRB-neutrino candidate figures in both analyses), it is noteworthy that the analysis here reported and the one reported in Ref. [26] both favor the same range of values of  $\eta$ . This might suggest that, if one were somehow able to combine the two analyses, then the overall evidence in favor of in-vacuo dispersion provided by presently-available IceCube data might be stronger than indicated by the individual statistical significance of each analysis. However, we do not yet see how such a combination of selection criteria could be achieved in a logically consistent manner, mostly because sharp knowledge of the GRB redshifts is a structural feature of the strategy of analysis advocated here.

We expect that the redshift-based strategy articulated in the previous sections will prove to be the best starting point for any future refinements, but we do not exclude that a suitable way may still be found for including GRBs whose redshift has not been measured (of course, from the perspective of our approach, somehow estimating the redshift of those GRBs with a suitably large uncertainty). Such a refinement of our approach could prove even more valuable in a few years, as more IceCube data is accrued and KM3NeT starts observing high-energy neutrinos.

At least equally important for the analysis of future IceCube and KM3NeT data would be to remove the other key limitation of our selection criteria, the restriction to shower-event neutrinos. This in principle could be achieved by incorporating the known [42] large and non-Gaussian probability distribution (whose peak lies sizably above the deposited energy) that relates the primary neutrino energy to the deposited energy in track events.

## ACKNOWLEDGMENTS

We thank Anastasia Tsvetkova for guidance on the available GRB catalogues and resources, which was very valuable in the early stages of our work on Appendix A. G.A.-C. and G.G. are grateful for financial support by the Programme STAR Plus, funded by Federico II University and Compagnia di San Paolo, and by the MIUR, PRIN 2017 grant 20179ZF5KS. G.R.’s work on this project was supported by the National Science Centre grant 2019/33/B/ST2/00050. G.D.’s work on this project was supported by the Research Council of Norway, project

number 301718. G.F.’s work on this project was supported by “Fondazione Angelo Della Riccia” and “The Foundation Blanceflor”. This work also falls within the scopes of the COST Action CA23130 “Bridging high and low energies in search of quantum gravity” and the COST Action CA18108 “Quantum Gravity phenomenology in the Multi-Messenger era”.

## Appendix A: Known-redshift GRB data

The following table contains the GRB data used in our analysis. We include all GRBs observed from January 2010 to December 2022 for which a definite redshift determination is available in the literature. We did not include GRBs with only upper and/or lower bounds on redshift. For the selection of the sample and the redshift values  $z$  we relied mostly on Greiner’s catalogue [33], referred to in our list as MP. Searching the literature for other GRBs whose redshift was measured, we found 24 which are not acknowledged as such in the summary table of Ref. [33]. For these GRBs we provide references to the relevant works and GCNs in the column “ $z$  ref.” of our table.

The angular data and the trigger times (TT) of the GRBs in our sample were downloaded from the web catalogue maintained by the IceCube collaboration [32], and were then manually checked against the primary GCN sources referred to in Greiner’s list [33]. If the right ascension (RA) or the declination (decl) values reported by [32] were no more than  $0.001^\circ$  off the best values we found in [33], we did not correct them, as our analysis is completely insensitive to errors of that order of magnitude. For the same reason, we do not provide the uncertainties affecting the angular positions, since we checked that they are all less than  $0.001^\circ$ . Accordingly, we report our angular values with three digital figures, with the understanding that the last one is affected by an uncertainty of order  $0.001^\circ$ .

TABLE I: List of GRBs with measured redshift

Name	RA ( $^\circ$ )	decl ( $^\circ$ )	TT (MJD)	$z$	$z$ ref.
GRB221226B	22.909	-41.527	59939.945	2.694	MP
GRB221110A	29.100	-27.294	59893.103	4.06	MP
GRB221009A	288.264	19.773	59861.553	0.151	MP
GRB221006A	337.246	15.714	59858.040	0.731	[43, 44]
GRB220813A	81.532	-33.016	59804.808	0.82	[45]
GRB220627A	201.369	-32.426	59757.890	3.084	MP
GRB220611A	66.515	-37.260	59741.751	2.3608	MP
GRB220527A	323.528	-14.972	59726.387	0.857	MP
GRB220521A	275.230	10.372	59720.972	5.6	MP
GRB220219B	240.914	31.234	59629.394	0.293	MP
GRB220117A	91.572	-28.437	59596.680	4.961	MP
GRB220107A	169.807	34.171	59586.615	1.246	MP
GRB220101A	1.353	31.769	59580.215	4.618	MP
GRB211227A	132.149	-2.735	59575.981	0.228	[46, 47]
GRB211211A	212.292	27.889	59559.549	0.073	[48, 49]
GRB211207A	149.624	-24.359	59555.870	2.272	MP



Name	RA (°)	decl (°)	TT (MJD)	z	z ref.	Name	RA (°)	decl (°)	TT (MJD)	z	z ref.
GRB211024B	154.713	24.568	59511.931	1.1137	MP	GRB181020A	13.982	-47.381	58411.792	2.938	MP
GRB211023B	170.310	39.136	59510.879	0.862	MP	GRB181010A	52.570	-23.038	58401.247	1.39	MP
GRB211023A	73.154	85.324	59510.546	0.39	MP	GRB180914B	332.356	25.062	58375.766	1.096	MP
GRB210919A	80.254	1.312	59476.020	0.2411	MP	GRB180805B	25.782	-17.494	58335.543	0.661	MP
GRB210905A	309.048	-44.440	59462.009	6.318	MP	GRB180728A	253.565	-54.044	58327.728	0.117	MP
GRB210822A	304.438	5.283	59448.388	1.736	MP	GRB180727A	346.666	-63.052	58326.594	2.0	MP
GRB210731A	300.305	-28.061	59426.931	1.2525	MP	GRB180720B	0.529	-2.919	58319.598	0.654	MP
GRB210722A	27.030	-6.347	59417.871	1.145	MP	GRB180703A	6.468	-67.179	58302.876	0.6678	MP
GRB210702A	168.578	-36.747	59397.797	1.16	MP	GRB180624A	318.098	-2.338	58293.576	2.855	MP
GRB210619B	319.718	33.850	59385.000	1.937	MP	GRB180620B	357.521	-57.962	58289.660	1.1175	MP
GRB210610B	243.918	14.399	59375.827	1.13	MP	GRB180618A	169.941	73.837	58287.030	0.544	MP
GRB210610A	204.282	14.465	59375.628	3.54	MP	GRB180510B	77.969	-62.324	58248.844	1.305	MP
GRB210517A	358.224	-39.102	59351.228	2.486	MP	GRB180418A	170.122	24.933	58226.281	1.55	MP
GRB210504A	222.392	-30.534	59338.580	2.077	MP	GRB180404A	83.548	-37.168	58212.032	1.0	MP
GRB210420B	254.325	42.570	59324.774	1.4	MP	GRB180329B	82.904	-23.690	58206.589	1.998	MP
GRB210411C	296.612	-39.398	59315.629	2.826	MP	GRB180325A	157.428	24.464	58202.078	2.25	MP
GRB210323A	317.947	25.369	59296.918	0.733	MP	GRB180314A	99.265	-24.496	58191.030	1.445	MP
GRB210321A	87.895	70.130	59294.301	1.487	MP	GRB180205A	126.820	11.542	58154.184	1.409	MP
GRB210312B	155.814	76.869	59285.870	1.069	MP	GRB180115A	12.039	-15.630	58133.178	2.487	MP
GRB210222B	154.606	-14.932	59267.943	2.198	MP	GRB171222A	148.278	35.627	58109.684	2.409	MP
GRB210210A	262.771	14.663	59255.084	0.715	MP	GRB171205A	167.415	-12.588	58092.306	0.0368	MP
GRB210204A	117.081	11.410	59249.270	0.876	MP	GRB171020A	39.248	15.204	58046.963	1.87	MP
GRB210116A	123.814	-5.867	59230.246	2.514	MP	GRB171010A	66.581	-10.463	58036.792	0.3293	MP
GRB210112A	219.006	33.054	59226.067	2.0	[50, 51]	GRB170903A	254.526	34.979	57999.534	0.886	MP
GRB210104A	103.772	64.676	59218.477	0.46	MP	GRB170817A	197.450	-23.381	57982.529	0.0093	MP
GRB201221D	171.059	42.144	59204.963	1.046	MP	GRB170728B	237.981	70.122	57962.961	1.27	MP
GRB201221A	214.480	-45.416	59204.298	5.7	MP	GRB170728A	58.888	12.182	57962.287	1.49	MP
GRB201216C	16.370	16.516	59199.963	1.1	MP	GRB170714A	34.350	1.991	57948.518	0.793	MP
GRB201104B	5.215	7.842	59157.732	1.954	MP	GRB170705A	191.704	18.307	57939.115	2.01	MP
GRB201103B	42.185	12.137	59156.755	1.105	MP	GRB170607A	7.366	9.243	57911.971	0.557	MP
GRB201024A	125.952	3.354	59146.117	0.999	MP	GRB170604A	342.656	-15.412	57908.798	1.329	MP
GRB201021C	12.529	-55.866	59143.852	1.07	MP	GRB170531B	286.884	-16.418	57904.918	2.366	MP
GRB201020B	75.470	77.068	59142.732	0.804	MP	GRB170519A	163.427	25.374	57892.215	0.818	MP
GRB201020A	261.228	31.428	59142.241	2.903	MP	GRB170428A	330.078	26.916	57871.384	0.454	MP
GRB201015A	354.319	53.416	59137.952	0.426	MP	GRB170405A	219.828	-25.243	57848.777	3.51	MP
GRB201014A	20.796	27.660	59136.950	4.56	MP	GRB170214A	256.341	-1.888	57798.649	2.53	MP
GRB200829A	251.205	72.329	59090.582	1.25	MP	GRB170202A	152.514	5.012	57786.769	3.645	MP
GRB200826A	6.786	34.027	59087.187	0.7481	MP	GRB170127B	19.977	-30.358	57780.634	2.2	MP
GRB200613A	153.042	45.754	59013.229	1.2268	MP	GRB170113A	61.733	-71.943	57766.420	1.968	MP
GRB200524A	213.043	60.905	58993.211	1.256	MP	GRB161219B	91.714	-26.792	57741.784	0.1475	MP
GRB200522A	5.682	-0.283	58991.487	0.554	MP	GRB161129A	316.228	32.135	57721.300	0.645	MP
GRB200411A	47.664	-52.318	58950.187	0.7	MP	GRB161117A	322.052	-29.614	57709.066	1.549	MP
GRB200219A	342.638	-59.120	58898.317	0.48	MP	GRB161108A	180.788	24.868	57700.148	1.159	MP
GRB200205B	107.788	-56.488	58884.807	1.465	MP	GRB161104A	77.894	-51.460	57696.404	0.79	MP
GRB191221B	154.830	-38.158	58838.861	1.148	MP	GRB161023A	311.022	-47.663	57684.944	2.708	MP
GRB191031D	283.289	47.644	58787.891	0.5	MP	GRB161017A	142.769	43.127	57678.744	2.013	MP
GRB191019A	340.025	-17.328	58775.634	0.248	MP	GRB161014A	332.648	7.469	57675.522	2.823	MP
GRB191011A	44.728	-27.845	58767.192	1.722	MP	GRB161001A	71.920	-57.261	57662.045	0.67	MP
GRB191004B	49.205	-39.634	58760.898	3.503	MP	GRB160821B	279.977	62.392	57621.937	0.16	MP
GRB190919B	311.877	-44.695	58745.991	3.225	MP	GRB160804A	221.630	9.999	57604.064	0.736	MP
GRB190829A	44.544	-8.958	58724.830	0.0785	MP	GRB160629A	4.863	76.967	57568.930	3.332	MP
GRB190719C	240.207	13.000	58683.624	2.469	MP	GRB160625B	308.598	6.919	57564.945	1.406	MP
GRB190627A	244.828	-5.289	58661.471	1.942	MP	GRB160624A	330.193	29.644	57563.477	0.483	MP
GRB190613A	182.529	67.235	58647.172	2.78	MP	GRB160623A	315.298	42.221	57562.208	0.367	MP
GRB190324A	49.616	-47.215	58566.947	1.1715	MP	GRB160509A	311.754	76.108	57517.374	1.17	MP
GRB190114C	54.505	-26.946	58497.873	0.42	MP	GRB160425A	280.327	-54.360	57503.977	0.555	MP
GRB190114A	65.544	2.192	58497.133	3.3765	MP	GRB160410A	150.685	3.478	57488.215	1.717	MP
GRB190106A	29.880	23.846	58489.566	1.859	MP	GRB160408A	122.625	71.128	57486.268	1.9	MP
GRB181201A	319.297	-12.631	58453.110	0.45	[52, 53]	GRB160327A	146.702	54.013	57474.386	4.99	MP
GRB181123B	184.367	14.598	58445.231	1.754	MP	GRB160314A	112.790	17.000	57461.481	0.726	MP
GRB181110A	302.318	-36.897	58432.364	1.505	MP	GRB160303A	168.701	22.742	57450.455	1.0	MP

Name	RA (°)	decl (°)	TT (MJD)	$z$	$z$ ref.	Name	RA (°)	decl (°)	TT (MJD)	$z$	$z$ ref.
GRB160228A	107.316	26.932	57446.732	1.64	MP	GRB140512A	289.370	-15.094	56789.814	0.725	MP
GRB160227A	194.808	78.679	57445.814	2.38	MP	GRB140509A	46.594	-62.639	56786.099	2.4	MP
GRB160203A	161.951	-24.789	57421.092	3.52	MP	GRB140508A	255.466	46.780	56785.128	1.0285	MP
GRB160131A	78.168	-7.050	57418.348	0.971	MP	GRB140506A	276.775	-55.636	56783.880	0.889	MP
GRB160121A	109.088	-23.592	57408.577	1.96	MP	GRB140430A	102.936	23.024	56777.857	1.6	MP
GRB160117B	132.195	-16.367	57404.583	0.87	MP	GRB140428A	194.368	28.385	56775.945	4.7	MP
GRB151229A	329.370	-20.732	57385.285	1.4	MP	GRB140423A	197.286	49.842	56770.355	3.26	MP
GRB151215A	93.584	35.516	57371.126	2.59	MP	GRB140419A	126.990	46.240	56766.171	3.956	MP
GRB151112A	2.054	-61.663	57338.573	4.1	MP	GRB140331A	134.864	2.717	56747.243	1.0	[57]
GRB151111A	56.845	-44.161	57337.356	3.5	MP	GRB140318A	184.089	20.209	56734.006	1.02	MP
GRB151031A	83.196	-39.122	57326.243	1.167	MP	GRB140311A	209.305	0.642	56727.879	4.952	MP
GRB151029A	38.528	-35.386	57324.326	1.423	MP	GRB140304A	30.643	33.474	56720.557	5.283	MP
GRB151027B	76.220	-6.450	57322.945	4.063	MP	GRB140301A	69.558	-34.257	56717.642	1.416	MP
GRB151027A	272.487	61.353	57322.166	0.81	MP	GRB140226A	221.492	14.993	56714.419	1.98	MP
GRB151021A	337.644	-33.197	57316.062	2.33	MP	GRB140213A	105.155	-73.137	56701.807	1.2076	MP
GRB150915A	319.658	-34.914	57280.888	1.968	MP	GRB140206A	145.334	66.761	56694.304	2.73	MP
GRB150910A	5.667	33.473	57275.378	1.359	MP	GRB140129B	326.757	26.206	56686.536	0.43	MP
GRB150831A	221.024	-25.635	57265.440	1.18	MP	GRB140114A	188.522	27.951	56671.498	3.0	MP
GRB150821A	341.913	-57.894	57255.406	0.755	MP	GRB131231A	10.590	-1.653	56657.198	0.642	MP
GRB150818A	230.356	68.342	57252.484	0.282	MP	GRB131229A	85.232	-4.396	56655.277	1.0	MP
GRB150728A	292.229	33.916	57231.536	0.46	MP	GRB131227A	67.378	28.883	56653.198	5.3	MP
GRB150727A	203.969	-18.325	57230.793	0.313	MP	GRB131117A	332.331	-31.762	56613.024	4.042	MP
GRB150616A	314.717	-53.394	57189.951	1.188	[54]	GRB131108A	156.502	9.662	56604.862	2.4	MP
GRB150518A	234.201	16.330	57160.904	0.256	MP	GRB131105A	70.967	-62.995	56601.087	1.686	MP
GRB150514A	74.876	-60.968	57156.774	0.807	MP	GRB131103A	348.919	-44.640	56599.922	0.599	MP
GRB150424A	152.306	-26.631	57136.321	1.0	[55, 56]	GRB131030A	345.067	-5.368	56595.872	1.293	MP
GRB150423A	221.579	12.284	57135.269	1.394	MP	GRB131011A	32.526	-4.411	56576.741	1.874	MP
GRB150413A	190.425	71.841	57125.580	3.139	MP	GRB131004A	296.113	-2.958	56569.904	0.717	MP
GRB150403A	311.505	-62.711	57115.913	2.06	MP	GRB130925A	41.179	-26.153	56560.164	0.347	MP
GRB150323A	128.178	45.465	57104.118	0.593	MP	GRB130907A	215.892	45.608	56542.902	1.238	MP
GRB150314A	126.670	63.834	57095.205	1.758	MP	GRB130831A	358.624	29.430	56535.545	0.4791	MP
GRB150301B	89.166	-57.970	57082.818	1.5169	MP	GRB130822A	27.922	-3.208	56526.663	0.154	MP
GRB150206A	10.074	-63.182	57059.604	2.087	MP	GRB130716A	179.574	63.053	56489.442	2.2	MP
GRB150120B	39.291	8.078	57042.307	3.5	MP	GRB130702A	217.312	15.774	56475.004	0.145	MP
GRB150120A	10.319	33.995	57042.123	0.46	MP	GRB130701A	357.229	36.100	56474.179	1.155	MP
GRB150101B	188.020	-10.934	57023.641	0.134	MP	GRB130615A	274.829	-68.161	56458.406	2.9	[54, 58]
GRB141225A	138.779	33.792	57016.959	0.915	MP	GRB130612A	259.794	16.720	56455.141	2.006	MP
GRB141221A	198.287	8.205	57012.338	1.452	MP	GRB130610A	224.420	28.207	56453.133	2.092	MP
GRB141220A	195.066	32.146	57011.252	1.3195	MP	GRB130606A	249.396	29.796	56449.878	5.91	MP
GRB141212A	39.125	18.147	57003.510	0.596	MP	GRB130604A	250.187	68.226	56447.288	1.06	MP
GRB141121A	122.669	22.217	56982.150	1.47	MP	GRB130603B	172.201	17.071	56446.659	0.356	MP
GRB141109A	144.531	-0.608	56970.243	2.993	MP	GRB130528A	139.505	87.301	56440.695	1.25	[59]
GRB141028A	322.602	-0.231	56958.455	2.33	MP	GRB130518A	355.668	47.465	56430.580	2.489	MP
GRB141026A	44.084	26.928	56956.109	3.35	MP	GRB130515A	283.440	-54.279	56427.056	0.8	MP
GRB141004A	76.734	12.820	56934.973	0.571	MP	GRB130514A	296.283	-7.976	56426.301	3.6	MP
GRB140930B	6.348	24.295	56930.821	1.465	MP	GRB130511A	196.646	18.710	56423.480	1.3033	MP
GRB140907A	48.146	46.605	56907.672	1.21	MP	GRB130505A	137.061	17.485	56417.349	2.27	MP
GRB140903A	238.014	27.603	56903.625	0.351	MP	GRB130427B	314.898	-22.546	56409.556	2.78	MP
GRB140808A	221.222	49.215	56877.037	3.29	MP	GRB130427A	173.137	27.699	56409.324	0.34	MP
GRB140801A	44.069	30.938	56870.792	1.32	MP	GRB130420A	196.106	59.424	56402.311	1.297	MP
GRB140713A	281.106	59.634	56851.780	0.935	MP	GRB130418A	149.037	13.667	56400.792	1.218	MP
GRB140710A	41.068	35.499	56848.428	0.558	MP	GRB130408A	134.405	-32.361	56390.911	3.758	MP
GRB140703A	12.996	45.102	56841.026	3.14	MP	GRB130215A	43.503	13.395	56338.063	0.597	MP
GRB140629A	248.977	41.877	56837.595	2.275	MP	GRB130131B	173.956	15.038	56323.799	2.539	MP
GRB140623A	225.473	81.191	56831.223	1.92	MP	GRB130131A	171.127	48.076	56323.581	1.55	MP
GRB140622A	317.173	-14.419	56830.400	0.959	MP	GRB121229A	190.101	-50.594	56290.209	2.707	MP
GRB140620A	281.871	49.731	56828.219	2.04	MP	GRB121226A	168.642	-30.406	56287.798	1.37	MP
GRB140614A	231.169	-79.129	56822.045	4.233	MP	GRB121217A	153.710	-62.351	56278.303	3.1	[60]
GRB140606B	328.125	32.015	56814.133	0.384	MP	GRB121211A	195.533	30.148	56272.574	1.023	MP
GRB140518A	227.252	42.418	56795.387	4.707	MP	GRB121209A	326.787	-8.235	56270.916	2.1	MP
GRB140515A	186.064	15.105	56792.384	6.32	MP	GRB121201A	13.467	-42.943	56262.518	3.385	MP

Name	RA (°)	decl (°)	TT (MJD)	$z$	$z$ ref.
GRB121128A	300.600	54.300	56259.212	2.2	MP
GRB121123A	307.318	-11.860	56254.419	2.7	[61, 62]
GRB121027A	63.598	-58.830	56227.314	1.773	MP
GRB121024A	70.472	-12.291	56224.122	2.298	MP
GRB120923A	303.795	6.221	56193.220	7.8	MP
GRB120922A	234.748	-20.182	56192.938	3.1	MP
GRB120909A	275.736	-59.449	56179.070	3.93	MP
GRB120907A	74.750	-9.315	56177.017	0.97	MP
GRB120815A	273.958	-52.131	56154.093	2.358	MP
GRB120811C	199.683	62.301	56150.649	2.671	MP
GRB120805A	216.538	5.825	56144.895	3.1	MP
GRB120804A	233.948	-28.782	56143.038	1.05	MP
GRB120802A	44.843	13.768	56141.334	3.796	MP
GRB120729A	13.074	49.940	56137.456	0.8	MP
GRB120724A	245.181	3.508	56132.277	1.48	MP
GRB120722A	230.497	13.251	56130.537	0.9586	MP
GRB120716A	313.051	9.599	56124.712	2.486	MP
GRB120714B	355.409	-46.184	56122.888	0.3984	MP
GRB120712A	169.588	-20.034	56120.571	4.17	MP
GRB120711A	94.678	-70.999	56119.114	1.405	MP
GRB120630A	352.296	42.556	56108.971	0.6	MP
GRB120624B	170.885	8.929	56102.930	2.1974	MP
GRB120521C	214.286	42.145	56068.974	6.0	MP
GRB120422A	136.910	14.019	56039.300	0.283	MP
GRB120404A	235.010	12.885	56021.535	2.876	MP
GRB120401A	58.082	-17.636	56018.225	4.5	[63]
GRB120327A	246.864	-29.415	56013.122	2.8115	MP
GRB120326A	273.905	69.260	56012.056	1.798	MP
GRB120311A	273.092	14.296	55997.232	0.35	[54]
GRB120305A	47.536	28.492	55991.818	0.225	MP
GRB120224A	40.942	-17.761	55981.194	1.1	MP
GRB120211A	87.754	-24.775	55968.499	2.4	MP
GRB120119A	120.029	-9.082	55945.170	1.728	MP
GRB120118B	124.871	-7.185	55944.709	2.943	MP
GRB111229A	76.287	-84.711	55924.943	1.3805	MP
GRB111228A	150.067	18.298	55923.656	0.714	MP
GRB111225A	13.155	51.572	55920.160	0.297	MP
GRB111215A	349.556	32.494	55910.586	2.06	MP
GRB111211A	153.090	11.208	55906.929	0.478	MP
GRB111209A	14.344	-46.801	55904.300	0.677	MP
GRB111129A	307.434	-52.713	55894.679	1.0796	MP
GRB111123A	154.846	-20.645	55888.759	3.1516	MP
GRB111117A	12.693	23.011	55882.510	2.211	MP
GRB111107A	129.478	-66.520	55872.035	2.893	MP
GRB111008A	60.451	-32.709	55842.926	5.0	MP
GRB111005A	223.282	-19.737	55839.337	0.0131	MP
GRB110918A	32.539	-27.105	55822.894	0.982	MP
GRB110818A	317.337	-63.981	55791.860	3.36	MP
GRB110808A	57.268	-44.194	55781.263	1.348	MP
GRB110801A	89.437	80.956	55774.826	1.858	MP
GRB110731A	280.504	-28.537	55773.465	2.83	MP
GRB110721A	333.659	-38.593	55763.200	0.382	[54, 64]
GRB110715A	237.684	-46.235	55757.551	0.82	MP
GRB110709B	164.654	-23.455	55751.898	2.109	MP
GRB110503A	132.776	52.208	55684.733	1.613	MP
GRB110422A	112.046	75.107	55673.654	1.77	MP
GRB110402A	197.402	61.253	55653.009	0.854	MP
GRB110213B	41.756	1.146	55605.605	1.083	MP
GRB110213A	42.964	49.273	55605.220	1.46	MP
GRB110205A	164.630	67.525	55597.085	2.22	MP
GRB110128A	193.896	28.065	55589.073	2.339	MP

Name	RA (°)	decl (°)	TT (MJD)	$z$	$z$ ref.
GRB110106B	134.154	47.003	55567.893	0.618	MP
GRB110106A	79.306	64.174	55567.643	0.093	[65]
GRB101225A	0.198	44.600	55555.776	0.847	MP
GRB101224A	285.924	45.714	55554.227	0.4536	MP
GRB101219B	12.231	-34.566	55549.686	0.5519	MP
GRB101219A	74.585	-2.540	55549.105	0.718	MP
GRB101213A	241.314	21.897	55543.451	0.414	MP
GRB100906A	28.684	55.630	55445.576	1.727	MP
GRB100905A	31.550	14.930	55444.631	7.9	MP
GRB100902A	48.629	30.979	55441.814	4.5	[66]
GRB100901A	27.264	22.759	55440.565	1.408	MP
GRB100816A	351.740	26.578	55424.026	0.8035	MP
GRB100814A	22.473	-17.995	55422.160	1.44	MP
GRB100728B	44.056	0.281	55405.439	2.106	MP
GRB100728A	88.758	-15.256	55405.095	1.567	MP
GRB100724A	194.543	-11.103	55401.029	1.288	MP
GRB100704A	133.642	-24.203	55381.149	3.6	[67]
GRB100628A	225.973	-31.664	55375.345	0.102	[68, 69]
GRB100625A	15.796	-39.088	55372.773	0.452	MP
GRB100621A	315.305	-51.106	55368.127	0.542	MP
GRB100615A	177.205	-19.481	55362.083	1.398	MP
GRB100606A	350.627	-66.241	55353.800	1.5545	[70]
GRB100518A	304.789	-24.554	55334.482	4.0	MP
GRB100513A	169.612	3.628	55329.088	4.772	MP
GRB100508A	76.246	-20.711	55324.389	0.5201	MP
GRB100425A	299.196	-26.431	55311.119	1.755	MP
GRB100424A	209.448	1.538	55310.689	2.465	MP
GRB100418A	256.362	11.462	55304.882	0.6235	MP
GRB100414A	192.112	8.693	55300.097	1.368	MP
GRB100413A	266.221	15.834	55299.732	3.9	[71]
GRB100316D	107.628	-56.256	55271.531	0.059	MP
GRB100316B	163.488	-45.473	55271.334	1.18	MP
GRB100316A	251.978	71.827	55271.099	3.155	MP
GRB100302A	195.516	74.590	55257.829	4.813	MP
GRB100219A	154.202	-12.566	55246.636	4.6667	MP
GRB100216A	154.251	35.522	55243.422	0.038	[72, 73]
GRB100213B	124.282	43.448	55240.957	0.604	[74, 75]
GRB100206A	47.163	13.157	55233.563	0.41	MP
GRB100117A	11.269	-1.595	55213.879	0.92	MP

## Appendix B: GRBs relevant for Figure 1

In this appendix we describe some properties of the GRB-neutrino events appearing in Fig. 1.

As already stressed in the main text, our analysis relied on the latest HESE neutrino data release by IceCube [31]. We considered only shower neutrinos, for which the energy is approximately equal to the observed-deposited energy [40, 42] (whereas the energy of track neutrinos is poorly known).

The GRBs which we analyzed (also in producing simulated data) are those of our catalogue reported in Appendix A. It is worth emphasizing that our catalogue agrees with both [32] and [33] for what concerns the four GRBs relevant for Fig. 1.

The neutrino with lowest energy among those relevant for Figure 1 has a deposited energy of 55.3 TeV and is

associated to GRB110503A [76], a long GRB ( $T_{90}=10.0$  s) with measured redshift of 1.613 [77].

The violet point in Fig. 1 is the one that was already taken into account in the analysis of [26], with deposited energy of 64.0 TeV, and is associated to GRB111229A [78], a long GRB ( $T_{90}=25.4$  s) with measured redshift of 1.38 [79].

The neutrino with deposited energy of 302.2 TeV which is relevant for Fig. 1 is associated to GRB120923A [80], a long GRB ( $T_{90}=27.2$  s) with measured redshift of 7.8 [81].

The highest energy neutrino relevant for Fig. 1 (also known as “big bird” [82]) has deposited energy of 2075.0 TeV and is associated with GRB120909A [83], a long GRB ( $T_{90}=112.1$  s) with measured redshift of 3.93 [84].

- 
- [1] M. G. Aartsen *et al.* *Science* **342** (2013), 1242856.  
 [2] R. Abbasi *et al.* *Science* **378** (2022), 538.  
 [3] T. Piran, *Phys. Rept.* **333** (2000), 529.  
 [4] E. Waxman and J. N. Bahcall, *Phys. Rev. Lett.* **78** (1997), 2292.  
 [5] P. Meszaros, *AIP Conf. Proc.* **428** (1998), 647.  
 [6] D. Guetta, D. Hooper, J. Alvarez-Muniz, F. Halzen and E. Reuveni, *Astropart. Phys.* **20** (2004), 429.  
 [7] M. Ahlers, M. C. Gonzalez-Garcia and F. Halzen, *Astropart. Phys.* **35** (2011), 87.  
 [8] G. Amelino-Camelia, J. R. Ellis, N. E. Mavromatos, D. V. Nanopoulos and S. Sarkar, *Nature* **393** (1998), 763.  
 [9] U. Jacob and T. Piran, *Nature Phys.* **3** (2007), 87.  
 [10] G. Amelino-Camelia and L. Smolin, *Phys. Rev. D* **80** (2009), 084017.  
 [11] R. Gambini and J. Pullin, *Phys. Rev. D* **59** (1999), 124021.  
 [12] J. Alfaro, H. A. Morales-Tecotl and L. F. Urrutia, *Phys. Rev. Lett.* **84** (2000), 2318.  
 [13] G. Amelino-Camelia and S. Majid, *Int. J. Mod. Phys. A* **15** (2000), 4301.  
 [14] R. C. Myers and M. Pospelov, *Phys. Rev. Lett.* **90** (2003), 211601.  
 [15] D. Mattingly, *Living Rev. Rel.* **8** (2005), 5.  
 [16] G. Amelino-Camelia, *Living Rev. Rel.* **16** (2013), 5.  
 [17] A. Addazi *et al.*, *Prog. Part. Nucl. Phys.* **125** (2022), 103948.  
 [18] G. Amelino-Camelia, L. Barcaroli, G. D’Amico, N. Loret and G. Rosati, *Phys. Lett. B* **761** (2016), 318.  
 [19] G. Amelino-Camelia, L. Barcaroli, G. D’Amico, N. Loret and G. Rosati, *Int. J. Mod. Phys. D* **26** (2017), 1750076.  
 [20] G. Amelino-Camelia, G. D’Amico, G. Rosati and N. Loret, *Nature Astron.* **1** (2017), 0139.  
 [21] Y. Huang and B. Q. Ma, *Communications Physics* **1** (2018), 62.  
 [22] Y. Huang, H. Li and B. Q. Ma, *Phys. Rev. D* **99** (2019), 123018.  
 [23] N. Aghanim *et al.* *Astron. Astrophys.* **641** (2020), A6 [erratum: *Astron. Astrophys.* **652** (2021), C4].  
 [24] V. Vasileiou, J. Granot, T. Piran and G. Amelino-Camelia, *Nature Phys.* **11** (2015), 344.  
 [25] G. Amelino-Camelia, D. Guetta and T. Piran, *Astrophys. J.* **806** (2015), 269.  
 [26] G. Amelino-Camelia, M. G. Di Luca, G. Gubitosi, G. Rosati and G. D’Amico, *Nature Astron.* **7** (2023), 996.  
 [27] S. Adrian-Martinez *et al.* *J. Phys. G* **43** (2016), 084001.  
 [28] M. G. Aartsen *et al.* *J. Phys. G* **48** (2021), 060501.  
 [29] T. Yuan, *Comput. Stat.* **36** (2021), 409.  
 [30] B. P. Abbott *et al.* *Astrophys. J. Lett.* **848** (2017), L13.  
 [31] IceCube Collaboration, “IceCube HESE 12-year data release”, <https://doi.org/10.7910/DVN/PZNO2T>, Harvard Dataverse, V2 (2023).  
 [32] P. Coppin, GRBweb, [https://icecube.wisc.edu/grbweb\\_public](https://icecube.wisc.edu/grbweb_public) (last retrieved on 08/08/2024).  
 [33] J. Greiner, <https://www.mpe.mpg.de/jcg/grbgen.html> (last retrieved on 08/08/2024).  
 [34] M. Ackermann, *et al.*, *Astrophys. J.* **741** (2011), 30.  
 [35] V. Vasileiou, A. Jacholkowska, F. Piron, J. Bolmont, C. Couturier, J. Granot, F. W. Stecker, J. Cohen-Tanugi and F. Longo, *Phys. Rev. D* **87** (2013) no.12, 122001.  
 [36] V. A. Acciari *et al.* *Phys. Rev. Lett.* **125** (2020), 021301.  
 [37] G. Fiorentini and G. Mezzorani, *Phys. Lett. B* **253** (1991), 181.  
 [38] J. Ludescher, A. Gozolchiani, M. I. Bogachev, A. Bunde, S. Havlin and H. J. Schellnhuber, *Proc. Natl. Acad. Sci. U.S.A.* **110** (2013), 11742.  
 [39] F. W. Stecker, S. T. Scully, S. Liberati and D. Mattingly, *Phys. Rev. D* **91** (2015), 045009.  
 [40] M. G. Aartsen *et al.* [IceCube], *JINST* **9** (2014), P03009.  
 [41] D. Colladay and V. A. Kostelecky, *Phys. Rev. D* **58** (1998), 116002.  
 [42] G. D’Amico, *Astropart. Phys.* **101** (2018), 8.  
 [43] R. O’Rourke Brogan *et al.*, *GCN Circ.* 32710 (2022).  
 [44] P. A. C. Cunha, *et al.*, *GCN Circ.* 32742 (2022).  
 [45] H. Faussey *et al.*, *GCN Circ.* 32471 (2022).  
 [46] D. B. Malesani *et al.*, *GCN Circ.* 31324 (2021).  
 [47] M. Ferro, *et al.*, *Astron. Astrophys.* **678** (2023), A142.  
 [48] A. J. Levan *et al.*, *GCN Circ.* 31235 (2021).  
 [49] J. C. Rastinejad, *et al.* *Nature* **612** (2022), 223.  
 [50] D. A. Kann *et al.*, *GCN Circ.* 29296 (2021).  
 [51] A. Hennessy, *et al.* *Mon. Not. Roy. Astron. Soc.* **526** (2023), 106.  
 [52] L. Izzo, *et al.*, *GCN Circ.* 23488 (2018).  
 [53] M. H. Siegel and J. K. Cannizzo, *GCN Circ.* 23499 (2018).  
 [54] J. Selsing, *et al.* *Astron. Astrophys.* **623** (2019), A92.  
 [55] N. R. Tanvir *et al.*, *GCN Circ.* 18100 (2015).  
 [56] F. Knust, *et al.*, *Astron. Astrophys.* **607** (2017), A84.  
 [57] A. Chrimes, E. Stanway, A. Levan, L. Davies, C. Angus and S. Greis, *Mon. Not. Roy. Astron. Soc.* **478** (2018), 2.  
 [58] J. Elliott *et al.*, *GCN Circ.* 14898 (2013).  
 [59] S. Jeong, *et al.*, *Astron. Astrophys.* **569** (2014), A93.  
 [60] J. Elliott, *et al.* *Astron. Astrophys.* **562** (2014), A100.  
 [61] S. Schmidl, *et al.*, *GCN Circ.* 13992 (2012).  
 [62] S. T. Holland, E. A. Helder, and D. Xu, *GCN Circ.* 14003 (2012).  
 [63] V. Sudilovsky *et al.*, *GCN Circ.* 13219 (2012).  
 [64] E. Berger, *GCN Circ.* 12193 (2011).  
 [65] S. Piranomonte *et al.*, *GCN Circ.* 11530 (2011).  
 [66] S. Campana *et al.*, *GCN Circ.* 11195 (2010).  
 [67] S. Campana and D. Grupe, *GCN Circ.* 10940 (2010).

- [68] S. B. Cenko *et al.*, GCN Circ. 10946 (2010).
- [69] A. Nicuesa Guelbenzu *et al.*, *Astron. Astrophys.* **583** (2015), A88.
- [70] T. Krühler *et al.* *Astron. Astrophys.* **581** (2015), A125.
- [71] S. Campana, P. A. Evans and S. T. Holland, GCN Circ. 10588 (2010).
- [72] J. R. Cummings *et al.* GCN Circ. 10428 (2010).
- [73] S. Dichiara, E. Troja, B. O'Connor, F. E. Marshall, P. Beniamini, J. K. Cannizzo, A. Y. Lien, T. Sakamoto, *Mon. Not. Roy. Astron. Soc.* **492** (2020), 5011.
- [74] A. Cucchiara *et al.*, GCN Circ. 10422 (2010).
- [75] Y. Li, J. Weston *et al.*, GCN Circ. 10913 (2010).
- [76] M. Stamatikos *et al.*, GCN Circ. 11991 (2011).
- [77] de Ugarte Postigo *et al.*, GCN Circ. 11993 (2011); D'Avanzo *et al.*, GCN Circ. 11997 (2011).
- [78] A. Y. Lien *et al.*, GCN Circ. 12774 (2011).
- [79] A. Cucchiara *et al.*, GRB Circ. 12777 (2011).
- [80] V. N. Yershov *et al.*, GCN Circ. 13796 (2012).
- [81] N. R. Tanvir *et al.*, *Astrophys. J.* **865** (2018), 107.
- [82] <https://icecube.wisc.edu/news/research/2014/05/growing-astrophysical-neutrino-signal-in-icecube-now-features-2-pev-neutrino/>
- [83] S. Immler *et al.*, GCN Circ. 13727 (2012).
- [84] O. E. Hartoog *et al.*, GCN Circ. 13730 (2012).